Actuator fault-tolerant active control of a quadcopter based on Backstepping Technique and Adaptive Observer

Abderrahim Ezzara, Ahmed Youssef Ouadine, Hassan Ayad

Actuator fault-tolerant active control of a quadcopter based on Backstepping Technique and Adaptive Observer

Abderrahim Ezzara[a]*, Ahmed Youssef Ouadine[b], Hassan Ayad[a]

[a]LSEET Laboratory, Department of Applied Physics, Faculty of Science and Technology, Cadi Ayyad university, Marrakesh, Morocco; [b]Ecole Royale de l'Air, Marrakesh, Morocco

ezzara.abderrahim@gmail.com (*Corresponding author) ayad.ha@gmail.com a.y.ouadine@gmail.com

ABSTRACT

This paper addresses the stabilization problem of an underactuated quadrotor UAV system in presence of actuator faults. First, a dynamic model of the quadcopter was established using a Lagrange approach. High-order non-holonomic constraints as well as different physical phenomena that can influence the dynamics of the structure have been taken into account. Then, for actuator faults, a new active fault tolerance strategy based on a backtracking approach and an adaptive observer is developed. The simulation results obtained illustrate the ability of the proposed control strategy to maintain performance and preserve stability in the event of actuator failures.

KEYWORDS

Active fault tolerant control, quadrotor unmanned aerial vehicles, nonlinear dynamical model, actuator faults, backstepping approach, adaptive observer.

1. Introduction

In light of increasing needs regarding automated systems availability, safety, and performance, it is necessary to develop a diagnostic module to detect faults that may damage these systems operations and identify their origin or source. Despite the tangible progress made, researchers must still deal with severe difficulties in controlling such systems, particularly in the presence of faults especially in the case of underactuated systems like unmanned aerial vehicles (UAV).

Quadcopters have been the subject of several studies in particular in the field of diagnosis and fault tolerance. (Baldini, et al. 2023 ; Najafi , et al. 2022 ; Ouadine, et al. 2020 ; Ren 2020 ; Xulin and Yuying 2018).

The work in (Avram, Zhang and Muse 2018) presents a nonlinear robust adaptive fault-tolerant altitude and attitude tracking scheme to accommodate actuator faults in a quadrotor. In (Xulin and Yuying 2018), the authors present a fuzzy active disturbance rejection control method for controlling a quadrotor UAV with actuator faults. An active fault-tolerant tracking control system approach for actuator faults on a quadrotor was discussed in (Zhong, et al. 2019). A fault-tolerant controller was designed on basis of adaptive estimation for actuator faults in (Hasanshahi, Ahmadi and Amjadifard 2019). In (Hong-Jun , et al. 2019), the authors present the diagnosis and compensation of sensors and actuators faults in a quadrotor UAV based on a nonlinear high-gain observer. Other strategies are proposed in (Lien, Chao-Chung and Yi-Hsuan 2020; Ren 2020; Yujiang , et al. 2018).

In the field of active fault-tolerant control (AFTC), observer-based reconstruction and fault estimation (FRE) has gained increased interest in the last two decades. Its advantage is that it can estimate the faults without going through the residual generation phase.

Significant literature on the subject of FE design methods for Lipschitz non-linear FTC systems has been established, mainly based on sliding-mode observers, observers for singular systems, and adaptive observers (Lan and Patton 2016). When faults are modelled in terms of parameter changes, adaptive observers can be used to estimate these faults.

This article presents a new active FTC technique on a quadrotor in the presence of actuator faults. It is based on a joint use of an adaptive observer for fault reconstruction and estimation and a backstepping approach for system control. Compared to previous work on the active FTC of a quadcopter UAV, in our work we have not neglected the non-linearity of the dynamic model of the quadcopter and the high-order non-holonomic constraints. It was used an adaptive observer proposed in (Oucief, Tadjine and Labiod 2016).

In the first section, the dynamic modelling of the quadcopter is carried out. To detect defects, an adaptive observer was developed to estimate the size of faults in the second section. Then, in the third section, a robust control strategy with actuator faults is established based on the backstepping technique and taking in to account the dynamic of faults. Finally, in the last section, simulations on MATLAB were carried out to validate the synthesized control laws. The results were conclusive in the presence of faults in the actuators.

2. Quadrotor Modelling

The aerial robot under study consists of a rigid cross frame coupled with four propellers, as illustrated in figure 1. The forward/ backward left/ right and the yaw movements are generated by a differential control strategy of the thrust delivered by each rotor. The up-down motion increases or reduces the overall thrust while keeping an equal individual thrust. To minimize the yaw drift induced by the responsive torques, the quadrotor aircraft is designed so that the set of rotors (right-left) spins clockwise and the set of rotors (front-rear) spins counter-clockwise.

Let E (O, X, Y, Z) designate an inertial frame, and B (o, x, y, z) designate a frame permanently coupled to the quadrotor, as illustrated in figure 1.

The absolute location is denoted by the three coordinates (x, y, z) and its attitude by the three Euler's angles (φ, θ, ψ) respectively called Roll angle (φ rotation around x-axis), Pitch angle (θ rotation around y-axis) and Yaw angle (ψ rotation around z-axis).

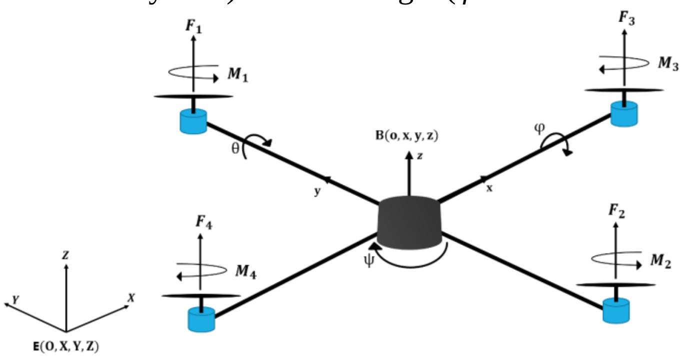

Figure 1. Quadrotor configuration

Literally, by using formalism of Newton-Euler, the quadrotor complete model (position and orientation dynamic) is provided as in (Bouadi, Tadjine and Bouchoucha 2007) by:

$$\ddot{\varphi} = \frac{1}{I_x}\left[\dot{\theta}\dot{\psi}\left(I_y - I_x\right) - K_{fax}\dot{\varphi}^2 - \mathrm{J}_r\overline{\Omega}\dot{\theta} + dU_2\right] \quad (1a)$$

$$\ddot{\theta} = \frac{1}{I_y}\left[\dot{\varphi}\dot{\psi}(I_z - I_x) - K_{fay}\dot{\theta}^2 - \mathrm{J}_r\overline{\Omega}\dot{\varphi} + dU_3\right] \quad (1b)$$

$$\ddot{\psi} = \frac{1}{I_z}\left[\dot{\theta}\dot{\varphi}\left(I_x - I_y\right) - K_{faz}\dot{\psi}^2 + K_dU_4\right] \quad (1c)$$

$$\ddot{x} = \frac{1}{m}\left[(C\varphi S\theta C\psi + S\varphi S\psi)U_1 - K_{ftx}\dot{x}\right] \quad (1d)$$
$$\ddot{y} = \frac{1}{m}\left[(C\varphi S\theta S\psi - S\varphi C\psi)U_1 - K_{fty}\dot{y}\right] \quad (1e)$$
$$\ddot{z} = \frac{1}{m}\left[(C\varphi C\theta)U_1 - K_{ftz}\dot{z}\right] - \mathrm{g} \quad (1f)$$

Where:

- Where C and S indicate the trigonometrical functions cos and sin respectively.
- m is the total mass of the quadrotor.
- K_p and K_d are lift and drag coefficients respectively.
- I_x, I_y and I_z are the constants inertia.
- K_{ftx}, $K_{fty}$and K_{ftz} are the translation drag coefficients.
- K_{fax}, $K_{fay}$and K_{faz} are the aerodynamic friction coefficients around (x, y, z).
- d is the distance between the quadrotor centre of mass and the rotation axis of propeller.
- J_r is the rotor inertia.

The quadrotor object of our study is (Draganfly IV: Manufactured by Draganfly Innovations). Parameter identification is studied in (Derafa, Madani and Benallegue 2006)

$K_P = 2.9842 \times 10^{-5}\ N.m/rad/s$	$m = 486$ g
$K_d = 3.2320 \times 10^{-5}$ N.m/rad/s	g $= 9.81\ m.s^{-2}$
$(I_x, I_y, I_z) = (3.8278, 3.8278, 7.1345) \times 10^{-3}\ {}^{N}\!/_{m.s^2}$	$d = 25\ cm$

$(K_{ftx}, K_{fty}, K_{ftz}) = (3.2, 3.2, 4.8) \times 10^{-2} N/m/s$

$(K_{fax}, K_{fay}, K_{faz}) = (5.5670\ , 5.5670\ , 6.3540) \times 10^{-4} N/rad/s$

$\mathrm{J}_r = 2.8385 \times 10^{-5}$ N.m/rad/$s^{\,2}$

U_1, U_2, U_3 and U_4 are the control inputs of the system which are written according to the angular velocities of the four rotors as follows:

$$\begin{bmatrix} U_1 \\ U_2 \\ U_3 \\ U_4 \end{bmatrix} = \begin{bmatrix} K_p & K_p & K_p & K_p \\ -K_p & 0 & K_p & 0 \\ 0 & -K_p & 0 & K_p \\ K_d & -K_d & K_d & -K_d \end{bmatrix} \begin{bmatrix} \omega_1^2 \\ \omega_2^2 \\ \omega_3^2 \\ \omega_4^2 \end{bmatrix} \quad (2)$$

$$\overline{\Omega} = \omega_1 - \omega_2 + \omega_3 - \omega_4 \quad (3)$$

From the equations of the translation dynamics in (1) we can deduce the expressions of the high-order nonholonomic constraints:

$$tan\theta = \frac{(\ddot{x} + \frac{K_{ftx}}{m}\dot{x})C\psi + (\ddot{y} + \frac{K_{fty}}{m}\dot{y})S\psi}{\ddot{z} + g + \frac{K_{ftz}}{m}\dot{z}} \quad \mathit{(4a)}$$

$$Sin\,\varphi = \frac{\left(\ddot{x} + \frac{K_{ftx}}{m}\dot{x}\right)S\psi - \left(\ddot{y} + \frac{K_{fty}}{m}\dot{y}\right)C\psi}{\sqrt{\left(\ddot{x} + \frac{K_{ftx}}{m}\dot{x}\right)^2 + \left(\ddot{y} + \frac{K_{fty}}{m}\dot{y}\right)^2 + \left(\ddot{z} + g + \frac{K_{ftz}}{m}\dot{z}\right)^2}} \quad (4b)$$

3. Nonlinear adaptive observer design

3. 1. State-space model

The complete model resulting by adding the actuator faults in the model (1) can be written in the state-space form:

$$\begin{aligned}\dot{x}(t) &= Ax(t) + \eta(y,u) + B\Phi(x,u) + Ef(x)\\ y(t) &= Cx(t)\end{aligned} \tag{5}$$

With:

$x(t) \in \mathbb{R}^n$ is the state vector of the system, such as:

$$x = [x_1, \dots, x_{12}]^T = \left[\varphi, \theta, \psi, x, y, z, \dot{\varphi}, \dot{\theta}, \dot{\psi}, \dot{x}, \dot{y}, \dot{z}\right]^T \tag{6}$$

$A \in \mathbb{R}^{n\times n}$, $B \in \mathbb{R}^{n\times s}$, $E \in \mathbb{R}^{n\times q}$ and $C \in \mathbb{R}^{p\times n}$ are known constant matrices.
$f(x) = \sigma(x) f_a(t)$, is the resultant vector of actuator faults related to quadrotor motions
$f_a(t) \in \mathbb{R}^r$ represent the actuators faults vector, with $f_a = [f_{a1},\ f_{a2}, f_{a3}, f_{a4}]^T$.
$\sigma(x)$: $\mathbb{R}^n \to \mathbb{R}^{q\times r}$ is a known function matrix which may depend nonlinearly on x.
$u(t) \in \mathbb{R}^m$ is the input control vector,
$y(t) \in \mathbb{R}^p$ is the output vector giving by $y = [\varphi, \theta, \psi, x, y, z]^T$.
$\eta(y,u)$ and $\Phi(x,u)$: are known nonlinear functions vectors.

Throughout this article, system model (5) satisfies the following conditions:
C0: The pair (C, A) is observable;
C1: The vector function $\eta(y,u)$ is continuous in its variables;
C2: $\Phi(x,u)$ and $\sigma(x)$ satisfy the Lipschitz property with respect to *x:* there exist positive constants γ_1 and γ_2 such that:

$$\| \Phi(x,u) - \Phi(\hat{x},u) \| \le \gamma_1 \| x - \hat{x} \| \tag{7a}$$

$$\| \sigma(x) - \sigma(\hat{x}) \| \le \gamma_2 \| x - \hat{x} \| \tag{7b}$$

C3: The fault vector f_a is piecewise constant and bounded in the following sense:

$$\|f_a(t)\| \le \left\|f_{a_m}\right\| = \gamma_3 \tag{8}$$

Where $f_{a_m} \in R^q$ is a known constant vector and γ_3 is a known positive constant.

3. 2. The adaptive state observer

The typical form of the adaptive state observer dealing with the class of nonlinear systems (5) is given by the following equations (Cho and Raramani 1995; That and Ding 2014):

$$\begin{aligned}\dot{\hat{x}}(t) &= A\hat{x}(t) + \eta(y,u) + B\Phi(\hat{x},u) + E\hat{f}(\hat{x}) + L\,(y - C\hat{x})\\ \dot{\hat{f}}(t) &= \rho^{-1}\sigma(\hat{x})^T FC(x - \hat{x})\end{aligned} \tag{9}$$

Where:
$\hat{x}$ and $\hat{f}(\hat{x}) = \sigma(\hat{x})\hat{f}_a(t)$ are the state and fault estimates.
L is the observer gain
ρ is a positive constant and
F is a matrix to be designed.

Under conditions C0, C1, C2 and C3 the state estimate $\hat{x}$ converges to the actual state x and $E\hat{f}(\hat{x})$ converges to $Ef(x)$, if there exist a symmetric positive definite matrix P and a matrix F such that (Cho and Raramani 1995):

$$E^T P = FC \tag{10}$$

Equality (10) is known as the observer matching condition (Floquet, Edwards and Spurgeon 2007),the equality $E^T P = FC$ hold if and only if (Corless and Tu 1998; Raoufi , Jose Marquez and Solo 2010):

$$rank(CE) = rank(E) \tag{11}$$

Unfortunately, the observer matching condition (10) is not satisfied for our system (5) and therefore we cannot use the adaptive observer of the form (9) to estimate x.
In (Oucief, Tadjine and Labiod 2016), authors have proposed a new methodology for an adaptive state observer design for a certain class of non-linear systems. This observer employs the nonlinear system model described by equation (5).

For developing the considered adaptive observer, in addition to conditions C0, C1, C2 and C3 the system model (5) has to satisfy the following conditions:
C4: The matrices A, B, E and C satisfy:

$$CB = 0_{p\times s} \tag{12a}$$

$$CE = 0_{p\times r} \tag{12b}$$

$$rank(CAE) = rank(E) \tag{12c}$$

C5: The first derivative in time of $\sigma(x)$ is continuous and bounded provided that x is bounded.

To satisfies the conditions C4, the state space (1) is rearranged. Considering the actuator faults, we obtain:

$$\begin{aligned}
\dot{x}_1 &= x_7 \\
\dot{x}_2 &= x_8 \\
\dot{x}_3 &= x_9 \\
\dot{x}_4 &= x_{10} \\
\dot{x}_5 &= x_{11} \\
\dot{x}_6 &= x_{12} \\
\dot{x}_7 &= a_1 x_8 x_9 + a_2 x_7^2 + a_3 \overline{\Omega} x_8 + b_1 (U_2 + f_{a1}) \\
\dot{x}_8 &= a_4 x_7 x_9 + a_5 x_8^2 + a_6 \overline{\Omega} x_7 + b_2 (U_3 + f_{a2}) \\
\dot{x}_9 &= a_7 x_7 x_8 + a_8 x_9^2 + b_3 (U_4 + f_{a3}) \\
\dot{x}_{10} &= a_9 x_{10} + U_x \frac{U_1}{m} \\
\dot{x}_{11} &= a_{10} x_{11} + U_y \frac{U_1}{m} \\
\dot{x}_{12} &= a_{11} x_{12} - \mathrm{g} + \frac{cos(x_1)\,cos(x_2)}{m} (U_1 + f_{a4})
\end{aligned} \tag{13}$$

With

$$a_1 = \frac{I_y - I_z}{I_x} \quad a_2 = \frac{-K_{fax}}{I_x} \quad a_3 = \frac{-\mathrm{J}_r}{I_x} \quad a_4 = \frac{I_z - I_x}{I_y} \quad a_5 = \frac{-K_{fay}}{I_y}$$

$$a_6 = \frac{\mathrm{J}_r}{I_y} \quad a_7 = \frac{I_x - I_y}{I_z} \quad a_8 = \frac{-K_{faz}}{I_z} \quad a_9 = \frac{-K_{fax}}{m} \quad a_{10} = \frac{-K_{fay}}{m}$$

$$a_{11} = \frac{-K_{faz}}{m} \quad b_1 = \frac{d}{I_x} \quad b_2 = \frac{d}{I_y} \quad b_3 = \frac{1}{I_z}$$

When these conditions are satisfied, a stable observer for the system (5) has the form (Oucief, Tadjine and Labiod 2016):

$$\dot{\hat{x}}(t) = A\hat{x}(t) + \eta(y,u) + B\Phi(\hat{x},u) + E\hat{f}(\hat{x}) + L\,(y - C\hat{x}) \tag{14a}$$

$$\hat{f}_a(t) = W + \Gamma \sigma^T(\hat{x}) H y \tag{14b}$$

$$\dot{W} = -\Gamma \frac{\mathrm{d}\sigma^T(\hat{x})}{\mathrm{d}t} H y - \Gamma \sigma^T(\hat{x}) [HC(A\hat{x}(t) + \eta(y,u)) + G\,(y(t) - C\hat{x}(t))] \tag{14c}$$

$\hat{f}(\hat{x}) = \sigma(\hat{x})\hat{f}_a(t)$, and $\hat{f}_a(t)$ is the unknown parameter vector.
H and G are constant matrices to be designed.
$\Gamma = \Gamma^T > 0$ is the learning rate matrix.

A sufficient condition for the asymptotic stability of the adaptive state observer is described in the following theorem (Oucief, Tadjine and Labiod 2016).

Theorem 1. Under conditions C0, C1, C2, C3, C4 and C5, the estimate of the state $\hat{x}$ converges to the real state *x* asymptotically while $E\hat{f}(\hat{x})$ converges to $Ef(x)$ if there are positive real constants ε_1 and ε_2 and matrices $P = P^T > 0$, H and G such that:

$$(A - LC)^T P + P(A - LC) + \varepsilon_1 PBB^T P + \varepsilon_2 PEE^T P + \varepsilon_1^{-1}{\gamma_1}^2 I_n + \varepsilon_2^{-1}{\gamma_2}^2{\gamma_3}^2 I_n < 0 \quad (15a)$$

$$HCA - GC = E^T P \quad (15b)$$

For our system, conditions C0 to C5 are satisfied, and as a consequence, the adaptation law (14) is feasible.

3. 3. Observer design

The objective is to synthesize an adaptive state observer corresponding to the model quadrotor given by (13) which can be described in the form of system given by (5).
Where:

$$\eta(y,u) = 0_{(12\times1)} \quad (16a)$$

$$\Phi(x,u) = \begin{bmatrix} a_1x_4x_6 & a_2x_2^2 & a_3\overline{\Omega}x_4 & b_1U_2 & a_4x_2x_6 & a_5x_4^2 & a_6\overline{\Omega}x_2 & b_2U_3 & a_7x_2x_4 \\ a_8x_6^2 & b_3U_4 & U_x\frac{U_1}{m} & U_y\frac{U_1}{m} & \frac{cos(x_1)cos(x_2)}{m}U_1 - \mathrm{g} \end{bmatrix}^T \quad (16b)$$

$$\sigma(x) = diag\left(b_1, b_2, b_3, \frac{cos(x_1)\cos(x_2)}{m}\right) \quad (16c)$$

We evaluate the Lipschitz constants of the individual rows of $\sigma(x)$:

$$\| \sigma(x) - \sigma(\hat{x}) \| \quad \leq \quad max\left(\left\|\frac{\mathrm{d}\sigma(x)}{\mathrm{d}x}\right\|\right) \| x - \hat{x} \| \quad (17)$$

We can take $\gamma_2 = 2.058$.

$\Phi(x,u)$ is locally Lipschitz, which means that its Lipschitz constant γ_1 depends on the region where the system operates. Suppose that the control input is chosen such that it keeps the state bounded in the set

$$\Omega_1 = \left\{ \begin{matrix} (x_1, x_2, x_3, x_4, x_5, x_6) \in \mathbb{R}^6 / \\ |x_1| < \frac{\pi}{2}, |x_2| < \frac{\pi}{2}, |x_3| < \pi, |x_4| < 5, |x_5| < 10, |x_6| < 20 \end{matrix} \right\} \quad (18)$$

Then $\Phi(x,u)$ can be extended into the bounded function $\Phi(sat(x))$which coincides with $\Phi(x,u)$ in Ω_1, and thus the system becomes globally Lipschitz (Farza, et al. 2009).

The computation of $\gamma_1$is given by:

$$\gamma_1 = max\left(\left\|\frac{\partial\Phi(sat(x))}{\partial x}\right\|\right) = 34.82 \quad (19)$$

For the calculation of γ_3, we assume that the maximum value that can be reached by the faults represents 50% of the setpoint indicated in (18). The computation of γ_3 is given by:

$$\gamma_3 = max(\|f_a(t)\|) = 10.18 \quad (20)$$

To find the observer gains, we can turn (15a) and (15b) into an LMI optimization problem.

Let $\varepsilon_1 = 76$ and $\varepsilon_2 = 80$. Using the Schur complement (Boyd, et al. 1994) for inequality (15a) we get:

$$\begin{bmatrix} \Lambda & PB & PE \\ B^T P & -\varepsilon_1^{-1} I_s & 0_{s\times q} \\ E^T P & 0_{q\times s} & -\varepsilon_2^{-1} I_q \end{bmatrix} < 0 \quad (21)$$

With:

$\Lambda = A^T P + PA - C^T M^T - MC + \varepsilon_1^{-1}\gamma_1^2 I_n + \varepsilon_2^{-1}\gamma_2^2\gamma_3^2 I_n$.

$M = PL$

Also, by using the same idea used in (Corless and Tu 1998) we can turn the problem of the resolution of equality (15b) into the following LMI optimization problem:
Minimize δ subject to:

$$\begin{bmatrix} \delta I_q & \Pi \\ \Pi^T & \delta I_n \end{bmatrix} \geq 0 \tag{22}$$

Where $\Pi = HCA - GC - E^T P$, and δ is a positive scalar.

Therefore, computing P,H, and G involves solving LMIs (21) and (22) for $P = P^T > 0$, $M = M^T$. LMIs were solved using MATLAB by a convex optimization tool (Grant and Boyd 2014). We get the following results:

$$\begin{aligned} & L = [L_1\; L_2]^T \\ & L_1 = 10^2 \times diag(7.6,7.6,6.1,1.6,1.6,3.9) \\ & L_2 = 10^5 \times diag(5.91,5.91,4.18,0.79,0.79,2.31) \\ & \Gamma = 9700\; \times I_4 \\ & \delta = 1.0001 \times 10^{-5} \end{aligned} \tag{23}$$

The unknown parameter vector estimates $\hat{f}_a(t)$ and conforming to (14) is then

$$\dot{\hat{f}}_a(t) = \Gamma \sigma^T(\hat{x}) E^T P e_x \tag{24a}$$

$$\dot{\hat{f}}_a(t) = \begin{bmatrix} \dot{\hat{f}}_{a1} \\ \dot{\hat{f}}_{a2} \\ \dot{\hat{f}}_{a3} \\ \dot{\hat{f}}_{a4} \end{bmatrix} = 10^3 \begin{bmatrix} 7.476e_7 - 1734.4e_1 \\ 7.474e_8 - 1733.9e_2 \\ 20.530e_9 - 3753.8e_3 \\ (0.621e_{12} - 57.34e_6)\, c\,x_1\, c\,x_2 \end{bmatrix} \tag{24b}$$

Where:
$e_x = x - \hat{x}$
$e_i = x_i - \hat{x}_i$ is the tracking-errors of x_i.
$c\,x_1 = cos(x_1)$ and $c\,x_2 = cos(x_2)$.

4. Control Strategy of Quadrotor with Actuator Faults

4. 1. Control Strategy

Generally, a fault-tolerant system is composed of two cascaded modules. The first one is a monitoring module which is used to detect faults, and diagnose their location and significance in a system. The second is a recovery module taking necessary actions so that the faulty system can achieve the control objectives almost at any time (Jain, J. Yamé and Sauter 2018).

In our case, an adaptive observer is used like a monitoring module (Figure 2) and the recovery module is based on the Backstepping approach.

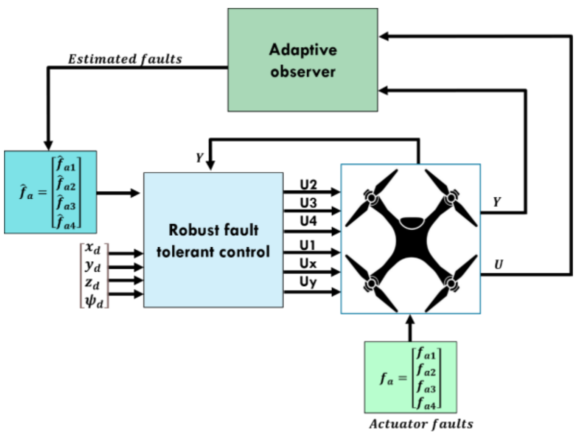

Figure 2. Fault-tolerant control system architecture

The following assumptions are needed for the analysis:

Assumption 1. The resultant of actuator faults related to quadrotor motions are slowly varying in time and bounded, as follows:

$$\begin{cases} \dot{f}(t)_{ai} \approx 0 \\ |f_{ai}(t)| \leq {f_{ai}}^{+} \end{cases} \quad i \in [1,2,3,4] \tag{25}$$

Where $\{{f_{a1}}^{+}, {f_{a2}}^{+}, {f_{a3}}^{+}, {f_{a4}}^{+}\}$ are positive constants.

Assumption 2. The unknown's parts $f(x, f_{ai}, t)$ including the resultants of actuator faults related to the quadrotor motions are also bounded:

$$|f(x, f_{ai}, t)| \leq |\sigma_i(x,t)| {f_{ai}}^{+} \leq k_{ai} \tag{26}$$

Where $\{k_{a1}, k_{a2}, k_{a3}, k_{a4}\}$ are positive constants.

The proposed control approach is based on two loops (internal and external loops). The internal loop has four control laws (roll, pitch, yaw, altitude). The external loop has two control laws of coordinates x and y.

The external control loop produces the desired roll (φ_d) and pitch (θ_d) via the corrective block given by equation (4). The corrective block has as a goal to correct the rotation of the roll and pitch based on the desired yaw (ψ_d). The synoptic scheme (Figure 3) below illustrates this control strategy:

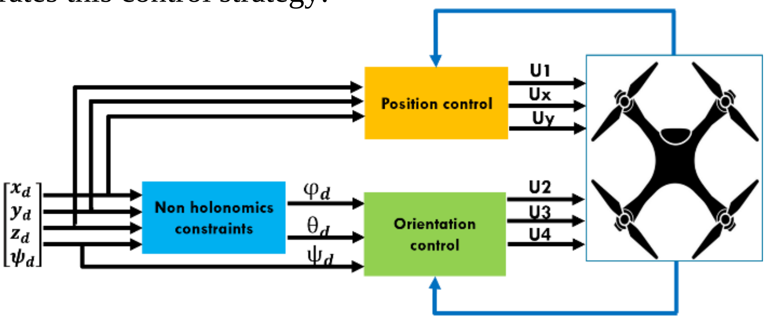

Figure 3. Synoptic scheme of the control strategy

4. 2. Control laws

Based on the backstepping technique, an iterative algorithm is used to synthesize the control laws forcing the system to follow the desired path in presence of actuator failures, we summarize all stages of calculation concerning the tracking errors and Lyapunov functions in the following way:

$$e_i = \begin{cases} x_{id} - x_i & i \in [1,2,3,4,5,6] \\ \dot{x}_{(i-6)d} + k_{(i-6)} e_{(i-6)} - x_i & i \in [7,8,9,10,11,12] \end{cases} \tag{27}$$
$$k_{(i-6)} > 0 \quad i \in [7,8,9,10,11,12]$$

The related Lyapunov functions are provided by:

$$V_i = \begin{cases} \frac{1}{2} e_i^2 & i \in [1,2,3,4,5,6] \\ V_{i-6} + \frac{1}{2} e_i^2 + e_x^T P e_x + e_f^T \Gamma^{-1} e_f & i \in [7,8,9,10,11,12] \end{cases} \tag{28}$$

The synthesized stabilizing control laws are as described in the following:

$$U_2 = \frac{1}{b_1} [\ddot{\varphi}_d + e_1 + k_7 e_7 + k_1(-k_1 e_1 + e_7) - a_1 x_8 x_9 - a_2 x_7^2 - a_3 \overline{\Omega} x_8 - \hat{f}_1(\hat{x})] \tag{29a}$$

$$U_3 = \frac{1}{b_2} [\ddot{\theta}_d + e_2 + + k_8 e_8 + k_2(-k_2 e_2 + e_8) - a_4 x_7 x_9 - a_5 x_8^2 - a_6 \overline{\Omega} x_7 - \hat{f}_2(\hat{x})] \tag{29b}$$

$$U_4 = \frac{1}{b_3}\left[\ddot{\psi}_d + e_3 + k_9 e_9 + k_3(-k_3 e_3 + e_9) - a_7 x_7 x_8 - a_8 x_9^2 - \hat{f}_3(\hat{x})\right] \tag{29c}$$

$$U_x = \frac{m}{U_1}\left[\ddot{x}_d + e_4 + k_{10} e_{10} + k_4(-k_4 e_4 + e_{10}) - a_9 x_{10}\right] \tag{29d}$$

$$U_y = \frac{m}{U_1}\left[\ddot{y}_d + e_5 + k_{11} e_{11} + k_5(-k_5 e_5 + e_{11}) - a_{10} x_{11}\right] \tag{29e}$$

$$U_1 = \frac{m}{cos(x_1)\,cos(x_2)}\left[\ddot{z}_d + e_6 + k_{12} e_{12} + k_6(-k_6 e_6 + e_{12}) - a_{11} x_{12} + \mathrm{g} - \hat{f}_4(\hat{x})\right] \tag{29f}$$

Where $\hat{f}_i(\hat{x}) = \sigma_i(\hat{x})\hat{f}_{ai}(t)$.

Proof. Considering the first subsystem:

$$\begin{cases} \dot{x}_1 = x_7 \\ \dot{x}_7 = a_1 x_8 x_9 + a_2 x_7^2 + a_3 \overline{\Omega} x_8 + b_1(U_2 + f_{a1}) \end{cases} \tag{30}$$

The corresponding reduced order observer is:

$$\begin{cases} \dot{\hat{x}}_1 = \hat{x}_7 + l_1(y_1 - \hat{y}_1) \\ \dot{\hat{x}}_7 = a_1 \hat{x}_8 \hat{x}_9 + a_2 \hat{x}_7^2 + a_3 \overline{\Omega} \hat{x}_8 + b_1(U_2 + \hat{f}_{a1}) + l_2(y_2 - \hat{y}_2) \end{cases} \tag{31}$$

The calculation of the command U_2 is done in two steps.

Step 1: For the first step we consider the first tracking-error e_1 given by

$$e_1 = x_{1d} - x_1 \tag{32}$$

Let the first Lyapunov function candidate:

$$V_1 = \frac{1}{2} e_1^2 \tag{33}$$

The time derivative of (33) is given by:

$$\dot{V}_1 = e_1 \dot{e}_1 = e_1(\dot{x}_{1d} - \dot{x}_1) = e_1(\dot{x}_{1d} - x_7) \tag{34}$$

According to Lyapunov's theorem, the stabilization of e_1 can be obtained by introducing a new virtual control $(x_7)_d$ which represent the desired value of x_7:

$$(x_7)_d = \alpha_1 = \dot{x}_{1d} + k_1 e_1 \quad (k_1 > 0) \tag{35}$$

The equation (34) is then:

$$\dot{V}_1 = -k_1 {e_1}^2 \leq 0 \tag{36}$$

Step 2: As x_7 is not a real command, we define the following tracking-error variable e_7 between the state variable x_7 and its desired value α_1

$$e_7 = \alpha_1 - x_7 = \dot{x}_{1d} + k_1 e_1 - x_7 \tag{37}$$

Let $e_x = x - \hat{x}$ and $e_f = f_a - \hat{f}_a$

Then, from (5), (14) and (25) we get:

$$\dot{e}_x = (A - LC)e_x + B\widetilde{\Phi} + E\left(\tilde{\sigma} f_a + \sigma(\hat{x})e_f\right) \tag{38a}$$

$$\dot{e}_f = -\Gamma \sigma^T(\hat{x})(HCA - GC)e_x \tag{38b}$$

Where $\tilde{\sigma} = \sigma(x) - \sigma(\hat{x})$ and $\widetilde{\Phi} = \Phi(x,u) - \Phi(\hat{x},u)$.

The augmented Lyapunov function is given by:

$$\begin{aligned} V_7 &= V_1 + \frac{1}{2} e_7^2 + e_x^T P e_x + e_f^T \Gamma^{-1} e_f \\ &= V_1 + \frac{1}{2} e_7^2 + V_{obs} \end{aligned} \tag{39}$$

The time derivative of V_7 is given by:

$$\dot{V}_7 = \dot{V}_1 + e_7 \dot{e}_7 + \dot{V}_{obs} \tag{40}$$

The time derivative of $V_{obs} = e_x^T P e_x + e_f^T \Gamma^{-1} e_f$ is given by:

$$\dot{V}_{obs} = 2 e_x^T P \dot{e}_x + 2 e_f^T \Gamma^{-1} \dot{e}_f \tag{41}$$

Substituting (38a) and (38b) into (41), we obtain

$$\dot{V}_{obs} = 2e_x^T P(A - LC)e_x + 2e_x^T PB\widetilde{\Phi} + 2e_x^T PE\tilde{\sigma} f_a + 2e_x^T PE\sigma(\hat{x})e_f - 2e_f^T \sigma^T(\hat{x})(HCA - GC)e_x \quad (42)$$

Using (15b), we get:

$$\dot{V}_{obs} = e_x^T[(A - LC)^T P + P(A - LC)]e_x + 2e_x^T PB\widetilde{\Phi} + 2e_x^T PE\tilde{\sigma} f_a \quad (43)$$

With $2u^T v \leq \varepsilon u^T u + \varepsilon^{-1} v^T v$, the Lipschitz conditions (7a) to (7b) and inequality (8), we obtain the following inequalities

$$\begin{aligned} 2e_x^T PB\widetilde{\Phi} &\leq \varepsilon_1 e^T{}_x PBBPe_x + \varepsilon_1{}^{-1} \widetilde{\Phi}^T \widetilde{\Phi} \\ &\leq \varepsilon_1 e_x PBBPe_x + \varepsilon_1{}^{-1} e^T{}_x \gamma_1{}^2 e_x \end{aligned} \quad (44)$$

and

$$\begin{aligned} 2e_x^T PE\tilde{\sigma} f_a &\leq \varepsilon_2 e^T{}_x PEEPe_x + \varepsilon_2{}^{-1} f_a{}^T \tilde{\sigma}^T \tilde{\sigma} f_a \\ &\leq \varepsilon_2 e^T{}_x PEEPe_x + \varepsilon_2{}^{-1} e_x{}^T \gamma_2{}^2 \gamma_3{}^2 e_x \end{aligned} \quad (45)$$

Where ε_1 and ε_2 are positive constants. Substituting (44) and (45) into (43), we obtain:

$$\dot{V}_{obs} \leq -e_x{}^T Q e_x \quad (46)$$

With: $Q = -[(A - LC)^T P + P(A - LC) + \varepsilon_1 PBB^T P + \varepsilon_2 PEE^T P + \varepsilon_1^{-1} \gamma_1{}^2 I_n + \varepsilon_2^{-1} \gamma_2{}^2 \gamma_3{}^2 I_n]$

Substituting (46) into (40) and replacing f_{a1} by his estimate $\hat{f}_{a1}$, (40) yields

$$\begin{aligned} \dot{V}_7 &\leq -k_1 e_1{}^2 + e_7[e_1 + \dot{e}_7] - e_x{}^T Q e_x \\ &\leq -k_1 e_1{}^2 - k_2 e_7{}^2 + e_7[k_2 e_7 + e_1 + \ddot{\varphi}_d + k_1(-k_1 e_1 + e_7) - a_1 x_8 x_9 \\ &\qquad - a_2 x_7^2 - a_3 \overline{\Omega} x_8 - b_1 U_2 - b_1 \hat{f}_{a1}] - e_x{}^T Q e_x \\ &\leq -k_1 e_1{}^2 - k_2 e_7{}^2 + e_7[k_2 e_7 + e_1 + \ddot{\varphi}_d + k_1(-k_1 e_1 + e_7) - a_1 x_8 x_9 \\ &\qquad - a_2 x_7^2 - a_3 \overline{\Omega} x_8 - b_1 U_2 - b_1 \hat{f}_{a1}] - c_1 \|e_x\|^2 \end{aligned} \quad (47)$$

Where $c_1 = \lambda_{min}(Q)$ ($\lambda_{min}(.)$ is the minimum eigenvalue of Q).

The stabilization of (e_1, e_7) can be obtained by introducing the input control U_2:

$$U_2 = \frac{1}{b_1}\left[\ddot{\varphi}_d + e_1 + k_2 e_7 + k_1(-k_1 e_1 + e_7) - a_1 x_8 x_9 - a_2 x_7^2 - a_3 \overline{\Omega} x_8 - b_1 \hat{f}_{a1}\right] \quad (48)$$

Finally, the equation (47) becomes

$$\dot{V}_7 \leq -k_1 e_1{}^2 - k_2 e_7{}^2 - c_1 \|e_x\|^2 \leq 0 \quad (49)$$

The same steps are followed to extract U_3, U_4, U_x, U_y and U_1.

5. Simulation Results

To evaluate the performance of the controller proposed in this work, we executed simulations in MATLAB. We carried out the simulations in two stages: A simulation with a healthy system (Test 1) and another simulation where we introduced faults on the actuators (Test 2).

Results of simulation without faults are shown in Figure 4, Figure 5.

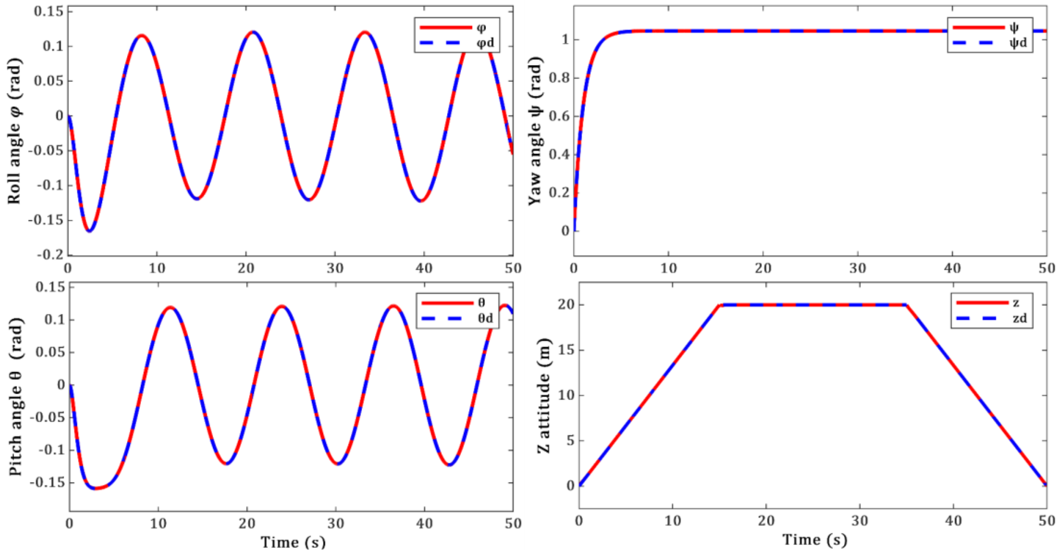

Figure 4. Trajectories along roll (φ), pitch (θ), yaw angle (ψ), and attitude Z in Test 1(without fault)

From this simulation (Figure 4), it can be seen that the desired and true state are matched perfectly, which clearly illustrates the good performance and robustness of the control strategy in absence of faults.

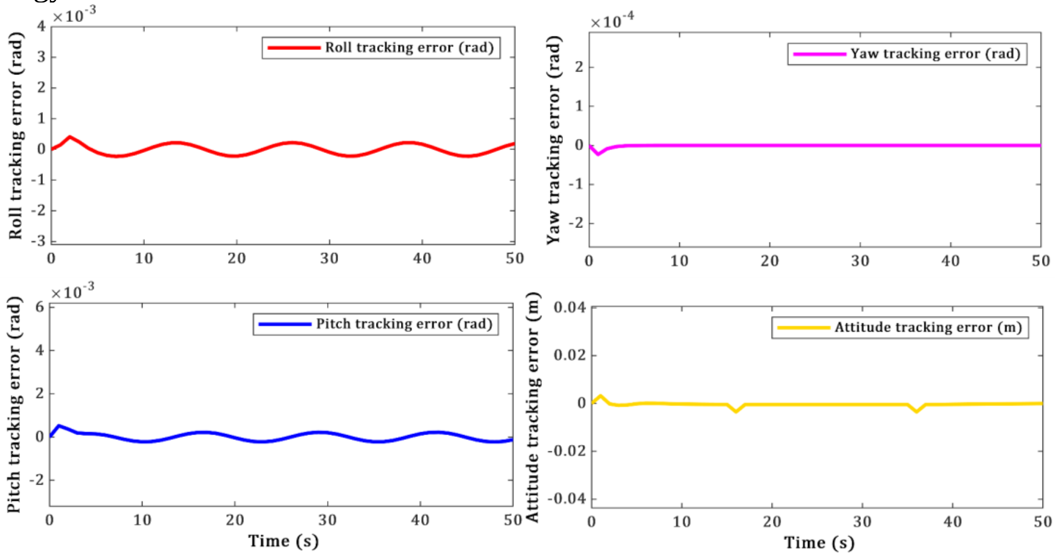

Figure 5. Tracking errors: roll (φ), pitch (θ), yaw angle (ψ), and attitude Z in Test 1 (without fault)

The estimation errors (Figure 5) quickly converge to 0 and remain below 10^{-3}, which clearly illustrates the good performance and robustness of the control system with the backstepping approach.

In the second simulation (Test 2), four actuator faults $\{f_{a1}, f_{a2}, f_{a3}, f_{a4}\}$ related to roll, pitch, yaw and altitude (φ, θ, ψ, z) commands are introduced. The simulation results are presented in Figure 6, 7, 8, 9,10 and 12.

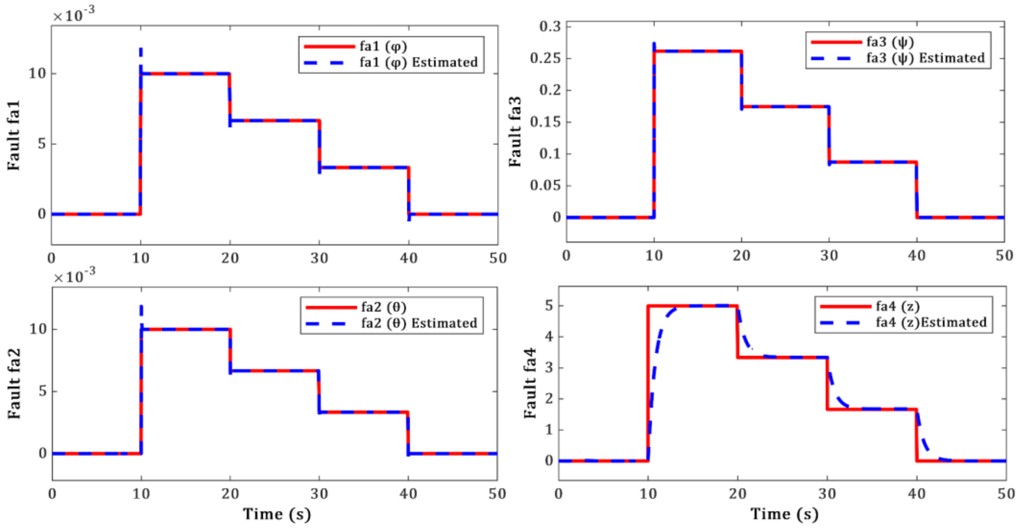

Figure 6. Fault estimation

According to Figure 6, there is very excellent estimation of the actuator faults. The estimates of f_{a1}, f_{a2} and f_{a3} converges rapidly to the real values. Meanwhile, the estimate of f_{a4} converge rapidly after a response time of around 2,5 s.

The mean of the estimation error of f_{a1}, f_{a2}, f_{a3} and f_{a4} respectively are 10^{-10}, 10^{-6}, 10^{-12} and 10^{-3}. Therefore, the proposed observer can give a fast and accurate fault estimation. We can also see that the estimate of the fault f_{a4} is not very precise when compared with the estimate of the other faults, this is due to the presence of non-linear terms in the fault dynamics of f_{a4}, which makes it more difficult to estimate.

The state estimates in faulty case are shown in Figure 7.

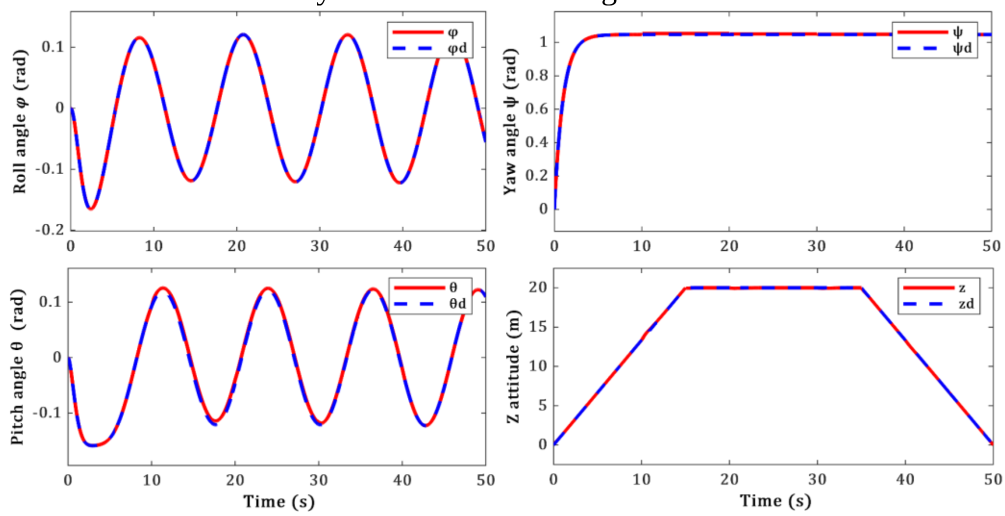

Figure 7. Trajectories along roll (φ), pitch (θ), yaw angle (ψ), and attitude Z axis (with actuators faults)

As shown in Figure. 7, trajectory tracking is very excellent even after the appearance of actuator faults. Small transient variations in the movements of roll, pitch, yaw and altitude at the instants of appearance of the faults at the instants:10s, 20s, 30s and 40s.

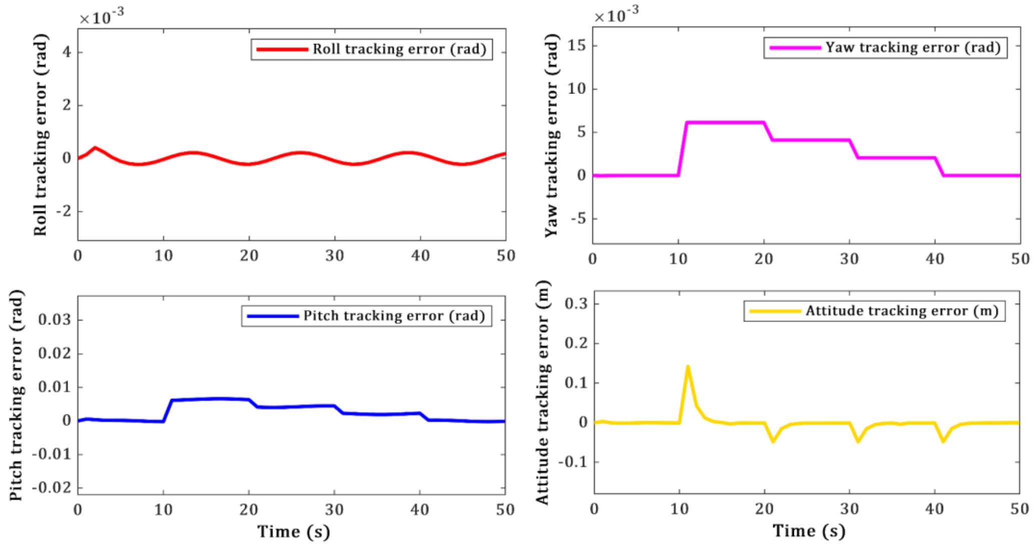

Figure 8. Tracking errors of roll (φ), pitch (θ), yaw angle (ψ), and Attitude Z (with actuators faults)

As shown in Figure 8, the roll (φ), pitch (θ) and yaw (ψ) estimation errors remain close to zero ($\approx 10^{-3}$). For the attitude estimation error z remains below 0.2 m which represents 2% of the desired attitude. Despite the faults, we can conclude that the trajectory tracking of our system is assured.

Figure 9 and Figure 10 illustrate the inputs control $\{U_1, U_2\ , U_3\ , U_4\}$ of our system. It is easy to notice the transient peaks (faulty case) in all controllers at the instants of appearance of the faults. Despite it, the stability of the closed-loop dynamics of the quadrotor is assured. Furthermore, we can observe input control signals provided by this control strategy are acceptable and physically realizable.

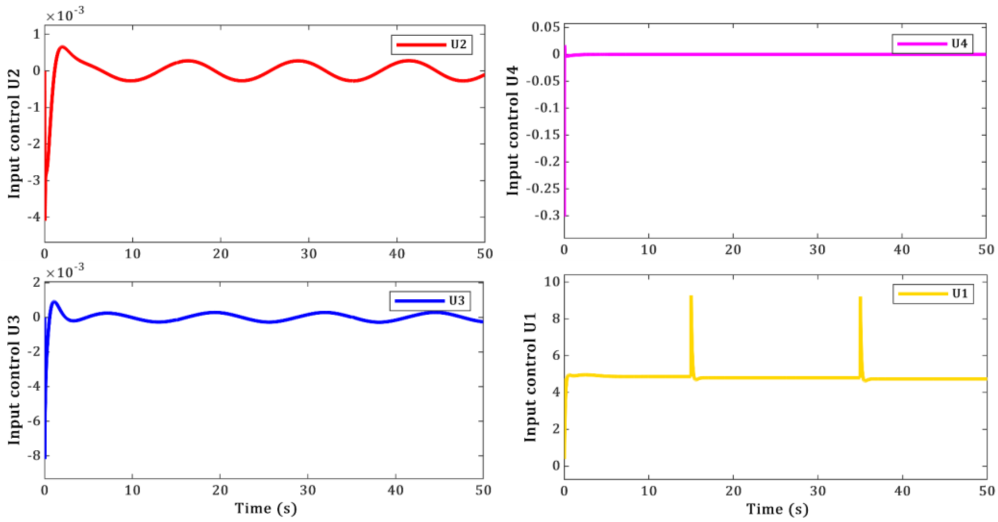

Figure 9. Control inputs of actuators in normal case (Without actuators faults)

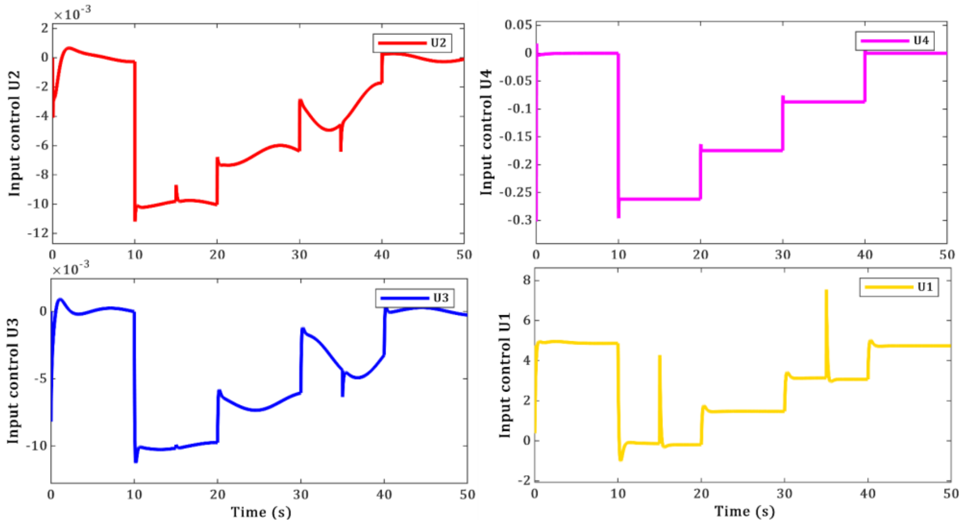

Figure 10. Control inputs of actuators in faulty case (with actuators faults)

To numerically evaluate the results obtained during the simulations, we will calculate two numerical criteria: the RMS error (Root Mean Square) and the average error of the desired coordinates. (Table 1).

Table 1. Numerical evaluation of the control strategy in Test 1 and Test 2

	RMS				**Error mean**			
	φ	θ	ψ	z	φ	θ	ψ	z
Test 1	$1{,}6.10^{-4}$	$1{,}8.10^{-4}$	$3{,}5.10^{-6}$	$9\,.10^{-4}$	$4{,}5.10^{-6}$	$1{,}2.10^{-5}$	$7{,}2\,.10^{-7}$	$3{,}8\,.10^{-4}$
Test 2	$1{,}6.10^{-4}$	$3{,}5.10^{-3}$	$3{,}4.10^{-3}$	$2{,}4.10^{-2}$	$4{,}5.10^{-6}$	$2{,}5.10^{-3}$	$2{,}4.10^{-3}$	$4\,.10^{-4}$

The quantitative analysis confirms that the proposed strategy not only ensures a satisfactory tracking performance of the state estimation but also preserves a low energy consumption with small control inputs.

Figure 11 and Figure 12 illustrate the 3D trajectory of the quadrotor aircraft throughout the flight. The simulation results indicate high performances and resilience towards stability and tracking even after the occurrence of actuator faults (Figure 12), which shows the efficacy of the control method suggested in this work.

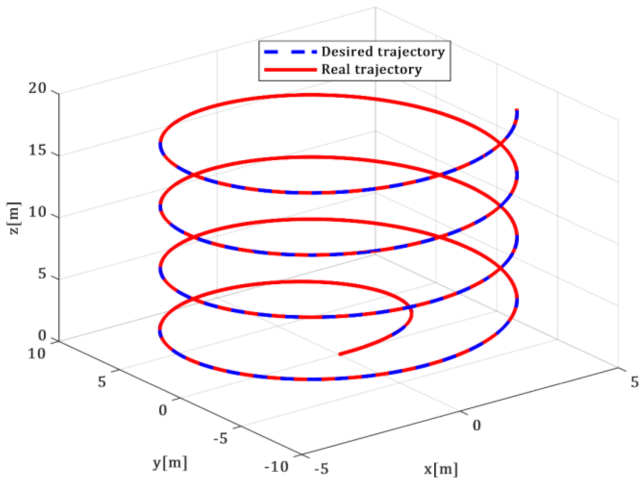

Figure 11. Global trajectory of the quadrotor in 3D along the (X, Y, Z) axis (Without faults)

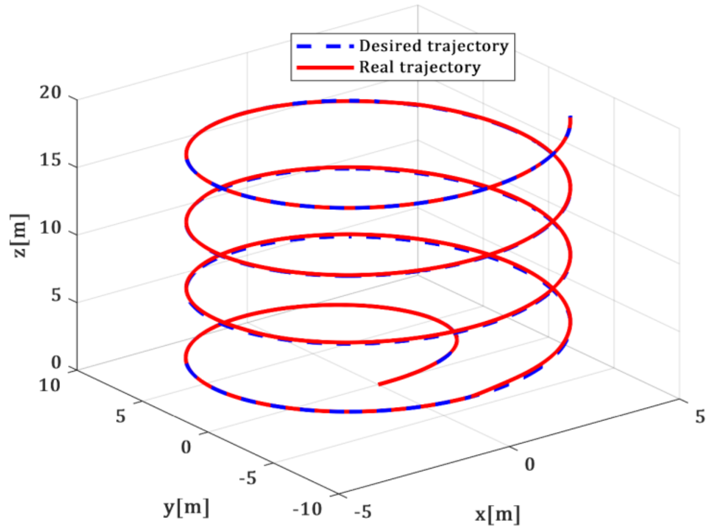

Figure 12. Global trajectory of the quadrotor in 3D along the (X, Y, Z) axis (with actuators faults)

6. Conclusion

This paper introduces a new fault-tolerant active control (FTC) strategy for diagnosing actuator faults in the quadcopter. This is the first time that this methodology proposed in *(Oucief, Tadjine and Labiod 2016)* is used in the field of active FTC for a quadrotor. It is based on the observer-based defect estimation and reconstruction (FRE) technique using an adaptive observer.

The contribution of this work is the use of a complete model of the quadrotor taking into consideration the nonlinearities and the high order nonholonomic constraints of the system which simulate a real behaviour of the quadrotor with actuators faults. The use of these observers makes it possible to estimate the additive and multiplicative defects regardless of the number of outputs measured.

Firstly, we introduced a complete nonlinear dynamical model of the quadrotor, taking into consideration several physics phenomena that might impact our system's navigation in space. Secondly, an adaptive observer has been developed to estimate simultaneously the system state used in feedback control and actuator faults used in the FDI task. Thirdly we presented a stabilizing control law, in the presence of actuator faults, based on backstepping technique.

Several simulations in MATLAB were run to evaluate the performance of the proposed strategy with a defective system at the roll, pitch, yaw and altitude actuators. The results of the simulation clearly illustrate the good performance of the adopted strategy. It made it possible to precisely estimate the faults and to ensure stability and the trajectory tracking. Moreover, we can observe that the input control signals provided by this control strategy are physically realizable.

Also,

References

Avram, Remus, Xiaodong Zhang, and Jonathan Muse. 2018. “Nonlinear Adaptive Fault-Tolerant Quadrotor Altitude and Attitude Tracking With Multiple Actuator Faults.” *IEEE Transactions on Control Systems Technology* 26 (2): 701–707. doi:10.1109/TCST.2017.2670522.

Baldini, Alessandro , Riccardo Felicetti, Alessandro Freddi, and Andrea Monteriù. 2023. “Fault-Tolerant Control of a Variable-Pitch Quadrotor under Actuator Loss of Effectiveness and Wind Perturbations.” *Sensors* 23 (10): 4907. doi:10.3390/s23104907.

Bouadi, Hakim, Mohamed Tadjine, and Mohamed Bouchoucha. 2007. “Modelling and stabilizing control laws design based on backstepping for an UAV type-quadrotor.” *IFAC Proceedings Volumes* 40 (15): 245-250. doi:10.3182/20070903-3-FR-2921.00043.

Boyd, Stephen, Laurent El Ghaoui, Eric Feron, and Venkataramanan Balakrishnan. 1994. *Linear Matrix Inequalities in System and Control Theory.* Philadelphia : Society for Industrial and Applied Mathematics.

Cho, Young Man, and Rajesh Raramani. 1995. “A Systematic Approach to Adaptive Observer Synthesis for Nonlinear Systems.” *Proceedings of Tenth International Symposium on Intelligent Control* 487-482. doi:10.1109/isic.1995.525102.

Corless, Martin, and Jay Tu. 1998. “State and Input Estimation for a Class of Uncertain Systems.” *Automatica* 34 (6): 757-764. doi:10.1016/S0005-1098(98)00013-2.

Derafa, Laloui , Tarek Madani, and Abdelaziz Benallegue. 2006. “Dynamic modelling and experimental identification of four rotor helicopter parameters.” *2006 IEEE International Conference on Industrial Technology* 1834-1839. doi:10.1109/ICIT.2006.372515.

Farza, Mondher, Mohammed M’SAAD, Tarek Maatoug, and Mohammed Kamoun. 2009. “Adaptive observers for nonlinearly parameterized class of nonlinear systems.” *Automatica* 45 (10): 2292-2299. doi:10.1016/j.automatica.2009.06.008.

Floquet, Thierry, Chris Edwards, and Sarah K Spurgeon. 2007. “On Sliding Mode Observers for Systems with Unknown Inputs.” *International Journal of Adaptive Control and Signal Processing* 21 (8-9): 638-656. doi:10.1002/acs.958.

Freddi, Alessandro, Sauro Longhi, and Andrea Monteriù. 2010. “Actuator fault detection system for a mini-quadrotor.” *IEEE International Symposium on Industrial Electronics* 2055-2060. doi:10.1109/ISIE.2010.5637750.

Grant, Michael, and Stephen Boyd. 2014. *CVX: Matlab Software for Disciplined Convex Programming.* March. Accessed 06 16, 2023. http://cvxr.com/cvx/.

Hasanshahi, Mahsa, Aliakbar Ahmadi, and Roya Amjadifard. 2019. “Robust Fault Tolerant Position Tracking Control for a Quadrotor UAV in Presence of Actuator Faults.” *Proceedings of the 2019 6th International Conference on Control, Instrumentation and Automation (ICCIA)* 1-6. doi:10.1109/ICCIA49288.2019.9030838.

Hong-Jun , Ma, Liu Yanli, Li Tianbo , and Yang Guang-Hong. 2019. “Nonlinear High-Gain Observer-Based Diagnosis and Compensation for Actuator and Sensor Faults in a Quadrotor Unmanned Aerial Vehicle.” *IEEE Transactions on Industrial Informatics* 15 (1): 550-562. doi:10.1109/TII.2018.2865522.

Jain, Tushar , Joseph J. Yamé, and Dominique Sauter. 2018. *Active Fault-Tolerant Control Systems-A Behavioral System Theoretic Perspective.* 1. Springer Cham. doi:10.1007/978-3-319-68829-9.

Lan, Jianglin, and Ron J. Patton. 2016. “Integrated fault estimation and fault-tolerant control for uncertain Lipschitz non-linear systems.” *International Journal of Robust and Nonlinear Control* 27 (5): 761-780. doi:10.1002/rnc.3597.

Lien, Yu-Hsuan, Peng Chao-Chung , and Chen Yi-Hsuan . 2020. “Adaptive Observer-Based Fault Detection and Fault-Tolerant Control of Quadrotors under Rotor Failure Conditions.” *Applied Sciences* 10 (10): 3503. doi:10.3390/app10103503.

Najafi , Amin , Mai The Vu, Saleh Mobayen, Jihad H. Asad, and Afef Fekih. 2022. “Adaptive Barrier Fast Terminal Sliding Mode Actuator Fault Tolerant Control Approach for Quadrotor UAVs.” *Mathematics* 10 (16): 3009. doi:10.3390/math10163009.

Ouadine , Ahmed Youssef , Mostafa Mjahed , Hassan Ayad , and Abdeljalil El Kari. 2020. “UAV Quadrotor Fault Detection and Isolation Using Artificial Neural Network and Hammerstein-Wiener Model.” *Studies in Informatics and Control* 29 (3): 317-328. doi:10.24846/v29i3y202005.

Oucief, Nabil , Mohamed Tadjine, and Salim Labiod . 2016. “A new methodology for an adaptive state observer design for a class of nonlinear systems with unknown parameters in unmeasured state dynamics.” *Transactions of the Institute of Measurement and Control* 40 (4): 1297-1308. doi:10.1177/0142331216680288.

Raoufi , Reza, Horacio Jose Marquez , and Alan Solo. 2010. “$\mathcal{H}\infty$ sliding mode observers for uncertain nonlinear Lipschitz systems with fault estimation synthesis.” *International Journal of Robust and Nonlinear Control* 20 (16): 1785-1801. doi:10.1002/rnc.1545.

Ren, Xiao-Lu. 2020. “Observer Design for Actuator Failure of a Quadrotor.” *IEEE Access* 8: 152742-152750. doi:10.1109/ACCESS.2020.3017522.

Stamnes, Oyvind Nistad, Ole Morten Aamo, and Glenn-Ole Kaasa. 2011. “Redesign of adaptive observers for improved parameter identification in nonlinear systems.” *Automatica* 47 (2): 403-410. doi:10.1016/j.automatica.2010.11.005.

Xulin, Liu, and Guo Yuying. 2018. “Fault tolerant control of a quadrotor UAV using control allocation.” *Proceedings of the 2018 Chinese Control And Decision Conference (CCDC)* 1818-1824. doi:10.1109/CCDC.2018.8407422.

Yujiang , Zhong, Zhang Youmin, Zhang Wei, Zuo Junyi, and Zhan Hao. 2018. “Robust Actuator Fault Detection and Diagnosis for a Quadrotor UAV With External Disturbances.” *IEEE Access* 6: 48169-48180. doi:10.1109/ACCESS.2018.2867574.

Zhong, Yu-jiang, Zhixiang Liu, Youmi Zhang, Wei Zhang, and Junyi Zuo. 2019. “Active fault-tolerant tracking control of a quadrotor with model uncertainties and actuator faults.” *Frontiers of Information Technology & Electronic Engineering* 20: 95-106. doi:10.1631/FITEE.1800570.